Available online at website: https://journal.bcrec.id/index.php/bcrec

Bulletin of Chemical Reaction Engineering & Catalysis, 19 (1) 2024, 118-125

Research Article

The Effect of Solvent on the Characteristics of FeBTC MOF as a Potential Heterogenous Catalyst Prepared via Green Mechanochemical Process

Indri Yati[1,*], Muhammad Ridwan[2], Franco Padella[3], Marzia Pentimalli[3,*]

[1]Research Center for Chemistry, National Research and Innovation Agency (BRIN), Kawasan Puspiptek, Serpong, Tangerang Selatan, 15314, Indonesia.
[2]Department of Chemistry, Faculty of Mathematics and Natural Sciences, Universitas Indonesia, Depok, West Java, 16424, Indonesia.
[3]Italian National Agency for New Technologies, Energy and Sustainable Economic Development (ENEA), via Anguillarese 301, Roma, 00123, Italy.

Received: 5th January 2024; Revised: 7th February 2024; Accepted: 8th February 2024
Available online: 11st February 2024; Published regularly: April 2024

Abstract

In this study, the synthesis of FeBTC (BTC = 1,3,5-benzenetricarboxylate) also known as MIL-100 (Fe) metal organic framework (MOF) has been carried out successfully using green mechanochemical method (neat grinding and liquid assisted grinding). The effect of solvent used in the synthesis was investigated for the first time to elucidate the physicochemical properties of FeBTC including crystal structure, thermal stability, pore size and specific surface area. The physicochemical properties of all FeBTC obtained in this study were compared to commercial FeBTC (Basolite F-300), characterized using powder X-Ray Diffraction (XRD), Thermogravimetric Analysis (TGA) and nitrogen physisorption isotherms. All Fe-BTC MOF synthesized in this study showed improved textural properties compared to commercial Basolite F-300 such as higher crystallinity, higher surface area and larger pore size. It was found that the best synthesis method was by using the mixture of ethanol and water with equal volume ratio as solvent. The highest BET surface area of FeBTC synthesized using this method was 972 m^2/g for FeBTC-EtOH/H_2O. This value is 2.3 times higher than the surface area of commercial Basolite F-300 (418 m^2/g). FeBTC with higher surface area is expected to have higher catalytic activity which makes this FeBTC an excellent candidate as a heterogenous catalyst for many reactions such as aldol condensation or esterification reaction.

Keywords: FeBTC MOF; MIL-100(Fe); Mechanochemical synthesis; Solvent effect; Heterogenous catalyst

How to Cite: I. Yati, M. Ridwan, F. Padella, M. Pentimalli (2024). The Effect of Solvent on the Characteristics of FeBTC MOF as a Potential Heterogenous Catalyst Prepared via Green Mechanochemical Process. *Bulletin of Chemical Reaction Engineering & Catalysis*, 19 (1), 118-125 (doi: 10.9767/bcrec.20115)

Permalink/DOI: https://doi.org/10.9767/bcrec.20115

1. Introduction

Metal-organic frameworks (MOF) are a class of crystalline materials constructed from metal ions or clusters linked together by organic ligands with strong covalent bonds forming a highly microporous framework [1,2]. Among various types of MOF, FeBTC (BTC = 1,3,5-benzenetricarboxylate) also known as MIL-100 (Fe) is one of the most promising materials due to extraordinary properties including high thermal stability, relatively strong acid sites, high porosity, and high specific surface area [3,4]. In contrast to most MOF which decompose upon moisture exposure, FeBTC is stable to moisture or hydrothermal condition and showed notable framework stability which is useful for adsorption application such as heavy metal adsorption or degradation of organic pollutants in water [5–11]. The nature of FeBTC is nontoxic which make them

---

* Corresponding Author.
Email: indriyati.1@brin.go.id (I. Yati);
marzia.pentimalli@enea.it (M. Pentimalli);
Telp: +62-21-7560929

potentially effective for drugs delivery [12,13]. FeBTC framework consist of a hybrid super tetrahedral structure build up from oxocentered trimmers of iron(III) octahedron which connected by 1,3,5-benzenetricarboxylate anions, forming mesoporous cages with diameter of 25 and 29 Å [14]. Activation of FeBTC by removing adsorbed water from the iron(III) octahedron creates coordinatively unsaturated metal sites which act as an electron acceptors or Lewis acid sites [15]. FeBTC has emerged as a highly active material for many catalysis reactions which required Lewis acid sites, including aldehydes acetylation, aldol condensation, esterification, isomerization and amine methylation [14,16–19].

FeBTC was firstly synthesized via solvothermal reaction which required high reaction temperature, high pressure condition, long reaction time and used large amounts of solvents [12]. Large scale synthesis for industrial application using solvothermal method seems to be ineffective. An alternative method to synthesize MOF is by using mechanochemical method which has advantage of high yield, rapid reaction time, room temperature and ambient pressure reaction condition, also requires no solvent in neat grinding method (NG) or little amount of solvent in liquid assisted grinding method (LAG) [20]. The mechanochemical method involved a friction or impact between solid reactant and milling balls resulting in high mechanical and thermal energy which induce the formation of reactive atom layers to initiate a chemical reaction without the need of external heating [21]. These makes the mechanochemical method a facile green synthesis method to overcome the extensive use of hazardous solvents in the conventional MOF synthesis and contributing to liquid wastes and energy consumption reduction [22].

For catalysis application, the synthesis method is crucial for targeting desired FeBTC properties such as crystal structure, pore dimension and surface areas to gain high catalytic activity. There are many synthesis factors that play significant roles in the MOF crystallization which will affect the overall MOF properties including solvent, pH of solution, reactant molar ratio and reaction temperature [23]. The effect of solvent has become a major concern because it regulates the coordination environment of metal ions and organic linkers, controlling organic linkers deprotonation, act as a directing agent and medium for the MOF crystal growth [24]. Conventional solvothermal method commonly uses polar organic solvents such as dimethylformamide or diethylformamide which may generate hazardous amines substance upon heating, contributing to MOF toxicity [25]. Green and environmentally friendly solvents have been explored in the solvothermal synthesis of MOF such as water, ethanol, and mixed solvent between water and ethanol [26–29]. Previous studies have shown that the mixture of ethanol and water in 1 to 1 ratio is the optimum solvent mixture for MOF synthesis such as iron and zirconium-based MOF [30–32]. The solvent mixture improves the self-assembly to produce small and uniform particle size.[30] In contrast, ethanol as single solvent decreased the nucleation rate thus aggregation rate becomes slow, producing large particle size [31,32]. In an industrial scale synthesis of MOF, the large amount use of ethanol as single solvent needs to be avoided because although it is considered as green solvent, the use of ethanol has some issues and competes with the extensive use of ethanol in medical, as fuel and as feedstock for other chemical production [33–35]. To the best of our knowledge, there has been no study reported on the effect of solvent in the synthesis of FeBTC via mechanochemical method. In fact, the mechanochemical synthesis of FeBTC has only been reported once by our group using tetramethyl ammonium hydroxide (TMAOH) aqueous solution as the solvent in LAG method [15]. The use of TMAOH as a base solvent has successfully produced high quality FeBTC. However, it is highly corrosive and may potentially produce toxic fumes. It also required more cautious handling under chemical fume hood.

In this study, we discussed the synthesis of FeBTC using iron chloride hexahydrate as iron source and trimesic acid as organic linker via mechanochemical method (NG and LAG). For the first time, the effect of green solvent used in the synthesis was evaluated to provide valuable insights on the physicochemical properties of FeBTC in terms of crystal structure, thermal stability, pore size and specific surface area. The physicochemical properties of all FeBTC obtained in this study were compared to commercial FeBTC

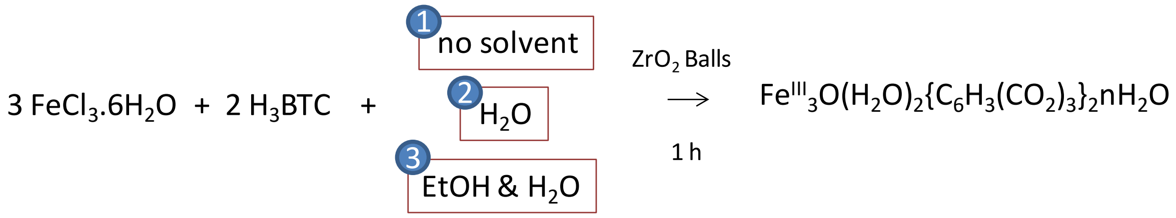

$$3\,FeCl_3.6H_2O + 2\,H_3BTC + \begin{array}{c}\boxed{\text{①}\ \text{no solvent}}\\ \boxed{\text{②}\ H_2O}\\ \boxed{\text{③}\ EtOH\ \&\ H_2O}\end{array} \xrightarrow[1\,h]{ZrO_2\ Balls} Fe^{III}_3O(H_2O)_2\{C_6H_3(CO_2)_3\}_2nH_2O$$

Figure 1. Reaction scheme of FeBTC preparation.

(Basolite F-300), characterized using powder X-Ray Diffraction (XRD), Thermogravimetric Analysis (TGA), and Nitrogen (N_2) physisorption isotherms.

2. Materials and Methods

2.1 Preparation of FeBTC

The FeBTC samples were synthesized at neutral pH by mixing 0.97 g of iron chloride hexahydrate ($FeCl_3.6H_2O$) as the iron source and 0.83 g of trimesic acid (H_3BTC) in Teflon lined stainless-steel reactor. Three different conditions were investigated as seen in Figure 1, where the first reaction was performed without any solvent addition (FeBTC-No Solvent), the second reaction was performed by adding 2 mL of distilled water into the reactor (FeBTC-H_2O) and the third reaction was using a mixture of 1 mL distilled water and 1 mL of ethanol (FeBTC- EtOH/H_2O). In these reactions, 21 zirconium oxide (ZrO_2) balls with diameter of 5 mm were used. The Teflon lined stainless-steel reactor was saturated by Argon and the milling action was carried out for one hour by using a SPEX 8000 ball milling apparatus (1425 rpm). A thick orange paste was collected and dried overnight under air at room temperature. The dried powder was then purified with ethanol by using Soxhlet extraction for 24 hours and washed three times with fresh ethanol using centrifuge until the solution was clear and then dried overnight at room temperature.

2.2 Characterizations

Powder X-ray diffraction (XRD) analysis was carried out using X-RED 3000 simultaneous diffractometer at 30 kV and 20 mA filament current using Fe-Kα radiation ($\lambda = 1.94$ Å). Specific surface area and pore size distribution was measured using NOVA 2000 sorptometer by N_2 physisorption at liquid nitrogen temperature (77 K). The specific surface area was determined using Brunauer-Emmet-Teller (BET) method and the pore size distribution was determined using Horvath-Kawazoe method. Thermogravimetry (TG) analysis was performed simultaneously using Perkin Elmer TG/DTA to analyze the thermal stability of all samples.

3. Result and Discussion

FeBTC MOF in this study were prepared by mechanochemical method with reaction conducted without solvent addition (FeBTC-No Solvent), with water as solvent (FeBTC-H_2O) and with mixture of ethanol and water in equal volume ratio as solvent (FeBTC-EtOH/H_2O). The crystal structures of these FeBTC were characterized using powder XRD analysis and the diffraction peaks were presented in Figure 2. Commercial sample of FeBTC, Basolite F-300 from BASF was analyzed using the same XRD instrument with our FeBTC samples and used as a standard reference. The XRD patterns of all the synthesized FeBTC samples are in good agreement with the characteristic peaks of Basolite F-300 as the standard reference, featuring strong diffraction peaks at 2θ: 13.6, 55.3, 64.7, and 98.5°. This result suggested that the MOF crystal formation of all FeBTC samples obtained under different reaction conditions is completed after one hour of Neat Grinding (NG) and Liquid-assisted Grinding (LAG) process. The samples obtained with mechanochemical process in this study have higher diffraction peaks intensity compared to commercial Basolite F-300, indicating a better crystallinity of MOF FeBTC structures. The FeBTC-EtOH/H_2O showed the highest diffraction peaks intensity compared to other samples, indicating that it has the best crystallinity among all samples. The crystallinity of each sample was calculated by comparing the area of crystalline peaks to the total area of all peaks (crystalline and amorphous). Basolite F-300, FeBTC-No Solvent, FeBTC-H_2O and FeBTC-EtOH/H_2O have crystallinity of 65, 70, 71, and 92 %, respectively. This result confirms that FeBTC-EtOH/H_2O has the highest crystallinity among other samples. The crystallite size of FeBTC samples calculated based on the highest peak using the Scherrer equation were found to be 66, 62, 62, and 59 nm for Basolite F-300, FeBTC-No Solvent, FeBTC-H_2O, and FeBTC-EtOH/H_2O, respectively. While Basolite F-300 has the largest crystallite size, FeBTC-EtOH/H_2O has the smallest crystallite size among all samples.

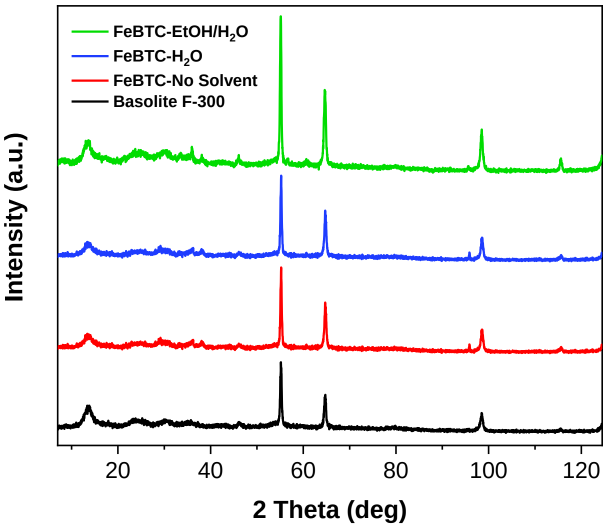

Figure 2. XRD pattern of commercial Basolite F-300 and FeBTC obtained without solvent addition (FeBTC-No Solvent), with water as solvent (FeBTC-H_2O) and with mixture of 1:1 water and ethanol as solvent (FeBTC-EtOH/H_2O), respectively.

TGA analysis was performed on all FeBTC samples to investigate the thermal stability of the samples as compared to the commercial Basolite F-300. The Basolite F-300 and FeBTC samples were heated at a constant rate of 10 °C/min under Argon from 25 to 600 °C. As seen in Figure 3, all FeBTC samples have the same thermal stability as the commercial Basolite F-300. All the samples are stable up to 330 °C and at higher temperature the structure collapses. Thermal decomposition data of Basolite F-300 and FeBTC samples obtained from TGA analysis was summarized in Table 1. The first weight loss of about 6–13 wt% which starts immediately after the heating up to 35 °C was due to a surface desorption of the slightly bound water molecules. The second weight loss of about 15 – 22 wt% that ends below 200 °C for Basolite F-300 and FeBTC-H_2O or below 330 °C for FeBTC-No Solvent and FeBTC-EtOH/H_2O, referred to the removal of the guest molecules and adsorbed solvents in the pore of all samples. Above 330 °C, a third weight loss begins and ends at about 480 °C with 33–50 wt% weight loss corresponds to the collapse of FeBTC frameworks and decomposition into iron oxide. All FeBTC samples synthesized in this study showed higher thermal stability compared to the one prepared through solvothermal method which showed thermal stability up to 270 °C [36].

In order to study the pore structures of FeBTC samples, N_2 physisorption isotherm were conducted at 77 K by previously degassing the samples overnight at 150 °C. The N_2 physisorption isotherms of commercial Basolite F-300 and the synthesized FeBTC samples are shown in Figure 4 and the N_2 physisorption isotherm data are summarized in Table 2. Meanwhile, the pore size distribution of Basolite F-300 and all the synthesized FeBTC samples were determined using H-K models are shown in Figure 5. It can be seen from Figure 4 that the N_2 physisorption isotherms of Basolite F-300 follows type I isotherms, indicating a microporous material. Meanwhile, the FeBTC-No Solvent, FeBTC-H_2O and FeBTC-EtOH/H_2O follows type I isotherm with small hysteresis indicating the presence of additional mesopore. It is interesting to note that all FeBTC samples have much higher BET surface

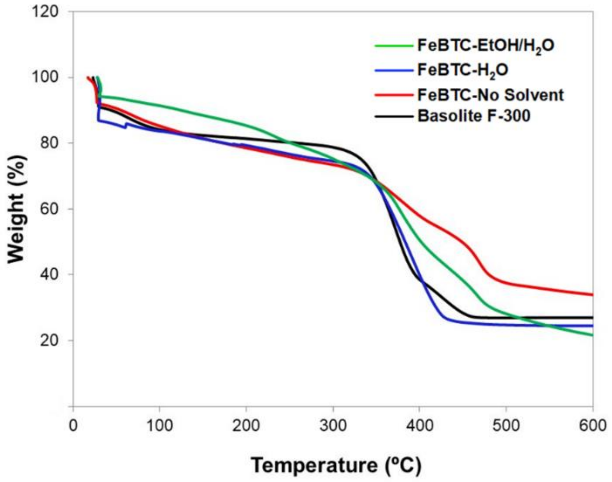

Figure 3. TGA curve of Basolite F-300 and FeBTC obtained without solvent addition (FeBTC-No Solvent), with water as solvent (FeBTC-H_2O) and with mixture of 1:1 water and ethanol as solvent (FeBTC-EtOH/H_2O), respectively.

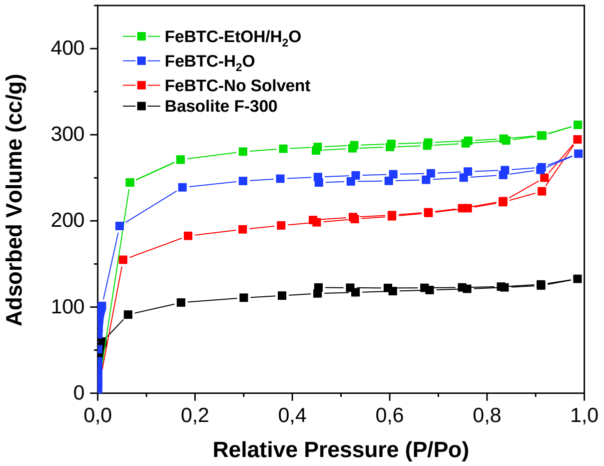

Figure 4. N_2 physisorption isotherm of Basolite F-300 and FeBTC obtained without solvent addition (FeBTC-No Solvent), with water as solvent (FeBTC-H_2O) and with mixture of 1:1 water and ethanol as solvent (FeBTC-EtOH/H_2O), respectively.

Table 1. Thermal decomposition data of Basolite F-300 and FeBTC samples obtained from TGA analysis.

Temperature (°C)	Weight Loss (%)				Inference
	Basolite F-300	FeBTC-No Solvent	FeBTC-H_2O	FeBTC-EtOH/H_2O	
<35	10	10	13	6	Surface desorption of water molecules
35–330	15	20	16	22	Removal of guest molecules and adsorbed solvents in the pore of all samples
330–480	50	33	45	43	Decomposition to iron oxide

areas and average pore size compared to the commercial basolite F-300 which has BET surface area of 418 m^2/g and average pore size of 6.4 Å. FeBTC-No Solvent has BET surface area of 650 m^2/g and average pore size of 7.2 Å. Meanwhile FeBTC-H_2O has higher BET surface area, which is 875 m^2/g and pore size of 7 Å. This is reasonable since the liquid assisted grinding (LAG) in ball milling method helps to improve the homogeneity during the reaction which resulted in a better crystallization and porosity of FeBTC. The highest BET surface area of 972 m^2/g was achieved by FeBTC-EtOH/H_2O, with pore size of 7.2 Å. The utilization of ethanol and water mixture as solvent improved the solubility of trimesic acid compared to the reaction using only water as solvent. Therefore, the exchange of ligand and carboxylates groups coordination with Fe becomes more favorable resulting in a better crystallization and pore structure of FeBTC samples [27].

In various applications of MOF including as an excellent candidate for heterogenous catalyst, the key parameter of the catalytic activity is strongly related to their crystal structures, the hybrid organic and inorganic intrinsic nature and more importantly their well define textural properties such as pore size and specific surface area [37]. All Fe-BTC MOF synthesized via mechanochemical method in this study have improved textural properties compared to commercial Basolite F-300. The FeBTC-EtOH/H_2O has outstanding properties including the highest crystallinity, highest BET surface areas and large pore size which make it more

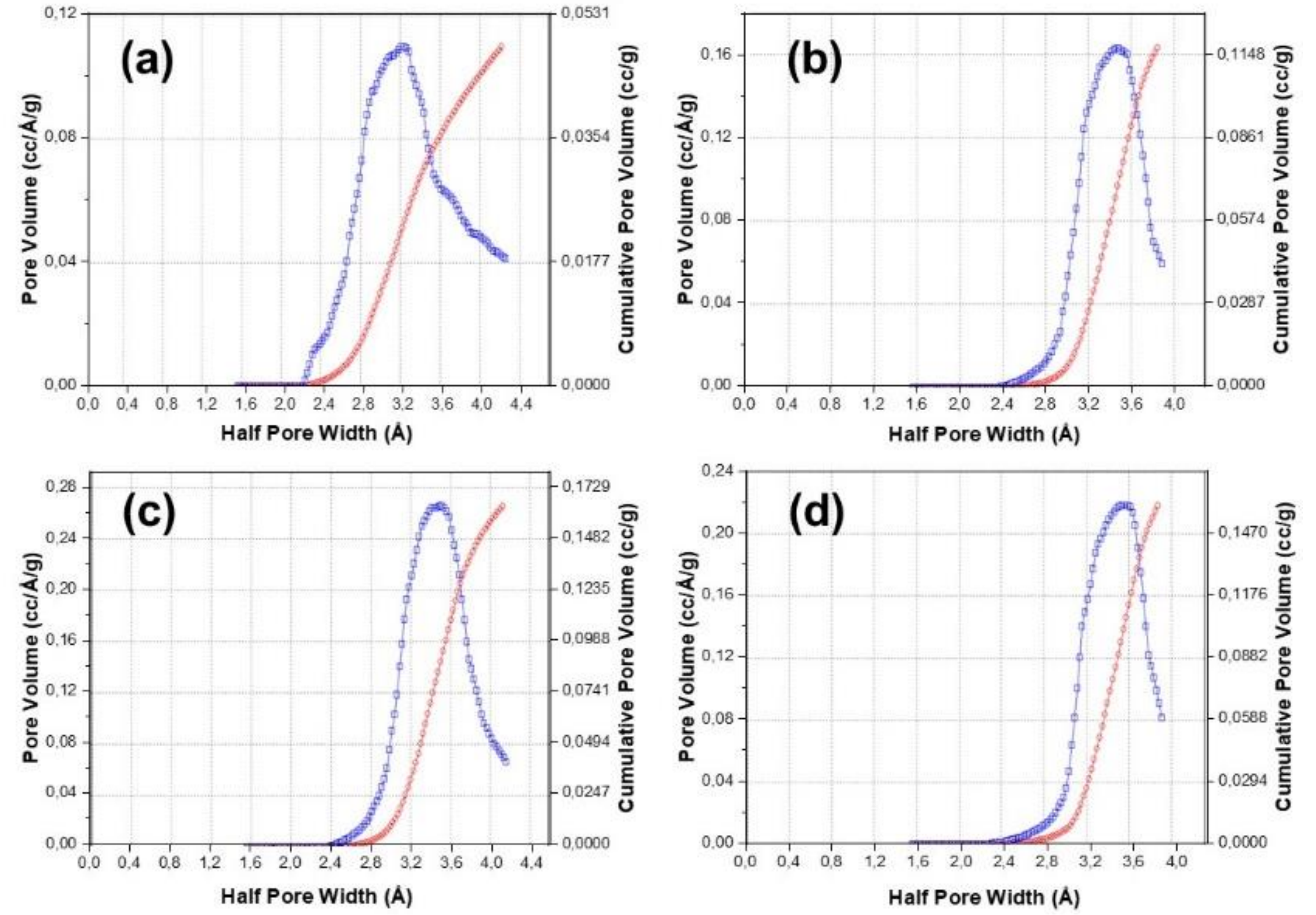

Figure 5. Pore size distribution (H-K models) of (a) Basolite F-300 and (b) FeBTC obtained without solvent addition (FeBTC-No Solvent), (c) with water as solvent (FeBTC-H_2O) and (d) with mixture of 1:1 water and ethanol as solvent (FeBTC-EtOH/H_2O), respectively.

Table 2. Summary data of N_2 physisorption of Basolite F-300 and FeBTC samples.

Catalysts	Basolite F-300	FeBTC-No Solvent	FeBTC-H_2O	FeBTC-EtOH/H_2O
Surface area (m^2/g)^a	418	650	875	972
Pore size (Å)^b	6.4	7.2	7.0	7.2

^{a}Surface area was calculated using Brunauer-Emmet-Teller (BET) method.
^{b}Pore size was calculated based on the pore size distributions (H-K models).

accessible for catalysis. A catalyst with higher surface area has more active sites for adsorption of reactant molecules thus increasing the catalytic activity [38]. FeBTC-EtOH/H_2O has 2.3 times higher BET surface area compared to commercial Basolite F-300. Therefore, it has great potential to be applied as a heterogeneous catalyst and expected to have higher catalytic activity compared to that of commercial Basolite F-300.

The key parameter of FeBTC-EtOH/H_2O surface area in this study was then compared to the reported reference in Table 3. The FeBTC-EtOH/H_2O has a higher surface area compared to Fe-BTC synthesized using solvothermal method for 12 h in sodium hydroxide aqueous solution and comparable surface area to SUST/Fe-BTC and Fe-BTC-24h which also synthesized using solvothermal method in sodium hydroxide aqueous solution with 24 h reaction time. FeBTC-EtOH/H_2O has only a slightly lower surface area compared to Fe-BTC synthesized using solvothermal method for 24 h in water. Compared to MFe_{LAG} synthesized using mechanochemical method in our previous study, FeBTC-EtOH/H_2O has comparable surface area. The findings in this study revealed that FeBTC-EtOH/H_2O prepared using green solvent via mechanochemical method has outstanding properties and surface area which comparable with other FeBTC prepared in conventional method. More importantly, the mechanochemical method employed for FeBTC synthesis in this study was more efficient, more environmentally friendly, and far less time consuming compared to those reported in the reference.

4. Conclusion

The synthesis of FeBTC metal organic framework using green mechanochemical method has been carried out successfully and the effect of different solvent system has been studied for the first time. All Fe-BTC MOF synthesized in this study have favorable textural properties compared to commercial Basolite F300 such as higher crystallinity, surface area and pore size. It was found that the best method to prepare the highest surface area of FeBTC is by using a solvent mixture of water and ethanol with 1:1 volume ratio. The FeBTC-EtOH/H_2O has the highest surface of 972 m^2/g and average pore size of 7.2 Å. The mechanochemical method employed for FeBTC synthesis in this study was more efficient, more environmentally friendly, and far less time consuming compared to conventional solvothermal method.

Acknowledgements

This work was funded by The Abdus Salam International Centre for Theoretical Physics (ICTP) through Training and Research in Italian Laboratories (TRIL) Fellowship Program and National Agency for New Technologies, Energy and Sustainable Economic Development (ENEA), Italy. This work was also supported by the 'RP-OR Nanoteknologi dan Material' grant funded by the National Research and Innovation Agency (BRIN), Indonesia. IY is the main contributor of this manuscript.

CRediT Author Statement

Indri Yati: Investigation, Formal analysis, Data curation, Writing – original draft, Writing – review & editing, Funding acquisition. *Muhammad Ridwan*: Writing-Review and Editing, Validation. *Franco Padella*: Methodology, Supervision, Writing – review & editing. *Marzia Pentimalli*: Methodology, Supervision, Writing – review & editing, Funding acquisition. All authors have read and agreed to the published version of the manuscript.

References

[1] O'Keeffe, M., Peskov, M.A., Ramsden, S.J., Yaghi, O.M. (2008). The Reticular Chemistry Structure Resource (RCSR) Database of, and Symbols for, Crystal Nets. *Accounts of Chemical Research*, 41 (12), 1782–1789. DOI: 10.1021/ar800124u.

[2] Guillerm, V., Kim, D., Eubank, J.F., Luebke, R., Liu, X., Adil, K., Lah, M.S., Eddaoudi, M. (2014). A supermolecular building approach for the design and construction of metal–organic frameworks. *Chemical Society Reviews*, 43(16), 6141–6172. DOI: 10.1039/C4CS00135D.

Table 3. Comparison of FeBTC-EtOH/H_2O surface area obtained in this study with reported reference.

Sample name	Synthesis Method	Reaction Time (h)	Solvent	Surface Area (m^2/g)	Ref.
SUST/Fe-BTC	Solvothermal	24	NaOH solution	1002	[6]
Fe-BTC	Solvothermal	12	NaOH solution	675	[26]
Fe-BTC-24h	Solvothermal	24	NaOH solution	1010	[39]
Fe-BTC	Solvothermal	24	H_2O	1125	[3]
MFe_{LAG}	Mechanochemical	1	TMAOH	1033	[15]
FeBTC-EtOH/H_2O	Mechanochemical	1	EtOH & H_2O	972	This work

[3] Hu, X., Lou, X., Li, C., Ning, Y., Liao, Y., Chen, Q., Mananga, E.S., Shen, M., Hu, B. (2016). Facile synthesis of the Basolite F300-like nanoscale Fe-BTC framework and its lithium storage properties. *RSC Advances*, 6(115), 114483–114490. DOI: 10.1039/C6RA22738D.

[4] Castañeda Ramírez, A.A., Rojas García, E., López Medina, R., Contreras Larios, J.L., Suárez Parra, R., Maubert Franco, A.M. (2021). Selective Adsorption of Aqueous Diclofenac Sodium, Naproxen Sodium, and Ibuprofen Using a Stable Fe3O4–FeBTC Metal–Organic Framework. *Materials*, 14(9) DOI: 10.3390/ma14092293.

[5] Zhang, H., Hu, X., Li, T., Zhang, Y., Xu, H., Sun, Y., Gu, X., Gu, C., Luo, J., Gao, B. (2022). MIL series of metal organic frameworks (MOFs) as novel adsorbents for heavy metals in water: A review. *Journal of Hazardous Materials*, 429, 128271. DOI: 10.1016/j.jhazmat.2022.128271.

[6] Martínez, F., Leo, P., Orcajo, G., Díaz-García, M., Sanchez-Sanchez, M., Calleja, G. (2018). Sustainable Fe-BTC catalyst for efficient removal of mehylene blue by advanced fenton oxidation. *Catalysis Today*, 313, 6–11. DOI: 10.1016/j.cattod.2017.10.002.

[7] Zhu, B.-J., Yu, X.-Y., Jia, Y., Peng, F.-M., Sun, B., Zhang, M.-Y., Luo, T., Liu, J.-H., Huang, X.-J. (2012). Iron and 1,3,5-Benzenetricarboxylic Metal–Organic Coordination Polymers Prepared by Solvothermal Method and Their Application in Efficient As(V) Removal from Aqueous Solutions. *The Journal of Physical Chemistry C*, 116(15), 8601–8607. DOI: 10.1021/jp212514a.

[8] Bezverkhyy, I., Weber, G., Bellat, J.-P. (2016). Degradation of fluoride-free MIL-100(Fe) and MIL-53(Fe) in water: Effect of temperature and pH. *Microporous and Mesoporous Materials*, 219, 117–124. DOI: 10.1016/j.micromeso.2015.07.037.

[9] Fang, Y., Yang, Z., Li, H., Liu, X. (2020). MIL-100(Fe) and its derivatives: from synthesis to application for wastewater decontamination. *Environmental Science and Pollution Research*, 27(5), 4703–4724. DOI: 10.1007/s11356-019-07318-w.

[10] Zhang, H., Hu, X., Li, T., Zhang, Y., Xu, H., Sun, Y., Gu, X., Gu, C., Luo, J., Gao, B. (2022). MIL series of metal organic frameworks (MOFs) as novel adsorbents for heavy metals in water: A review. *Journal of Hazardous Materials*, 429, 128271. DOI: 10.1016/j.jhazmat.2022.128271.

[11] Delpiano, G.R., Tocco, D., Medda, L., Magner, E., Salis, A. (2021). Adsorption of Malachite Green and Alizarin Red S Dyes Using Fe-BTC Metal Organic Framework as Adsorbent. *International Journal of Molecular Sciences*, 22(2) DOI: 10.3390/ijms22020788.

[12] Horcajada, P., Chalati, T., Serre, C., Gillet, B., Sebrie, C., Baati, T., Eubank, J.F., Heurtaux, D., Clayette, P., Kreuz, C., Chang, J.-S., Hwang, Y.K., Marsaud, V., Bories, P.-N., Cynober, L., Gil, S., Férey, G., Couvreur, P., Gref, R. (2010). Porous metal–organic-framework nanoscale carriers as a potential platform for drug delivery and imaging. *Nature Materials*, 9(2), 172–178. DOI: 10.1038/nmat2608.

[13] Quijia, C.R., Lima, C., Silva, C., Alves, R.C., Frem, R., Chorilli, M. (2021). Application of MIL-100(Fe) in drug delivery and biomedicine. *Journal of Drug Delivery Science and Technology*, 61, 102217. DOI: 10.1016/j.jddst.2020.102217.

[14] Dhakshinamoorthy, A., Alvaro, M., Horcajada, P., Gibson, E., Vishnuvarthan, M., Vimont, A., Grenèche, J.-M., Serre, C., Daturi, M., Garcia, H. (2012). Comparison of Porous Iron Trimesates Basolite F300 and MIL-100(Fe) As Heterogeneous Catalysts for Lewis Acid and Oxidation Reactions: Roles of Structural Defects and Stability. *ACS Catalysis*, 2(10), 2060–2065. DOI: 10.1021/cs300345b.

[15] Pilloni, M., Padella, F., Ennas, G., Lai, S., Bellusci, M., Rombi, E., Sini, F., Pentimalli, M., Delitala, C., Scano, A., Cabras, V., Ferino, I. (2015). Liquid-assisted mechanochemical synthesis of an iron carboxylate Metal Organic Framework and its evaluation in diesel fuel desulfurization. *Microporous and Mesoporous Materials*, 213, 14–21. DOI: 10.1016/j.micromeso.2015.04.005.

[16] Liu, F., Ma, X., Li, H., Wang, Y., Cui, P., Guo, M., Yaxin, H., Lu, W., Zhou, S., Yu, M. (2020). Dilute sulfonic acid post functionalized metal organic framework as a heterogeneous acid catalyst for esterification to produce biodiesel. *Fuel*, 266, 117149. DOI: 10.1016/j.fuel.2020.117149.

[17] Li, H., Wang, J., Ma, X., Wang, Y., Li, G., Guo, M., Cui, P., Lu, W., Zhou, S., Yu, M. (2021). Carbonized MIL−100(Fe) used as support for recyclable solid acid synthesis for biodiesel production. *Renewable Energy*, 179, 1191–1203. DOI: 10.1016/j.renene.2021.07.122.

[18] Dhakshinamoorthy, A., Alvaro, M., Chevreau, H., Horcajada, P., Devic, T., Serre, C., Garcia, H. (2012). Iron(iii) metal–organic frameworks as solid Lewis acids for the isomerization of α-pinene oxide. *Catal. Sci. Technol.*, 2(2), 324–330. DOI: 10.1039/C2CY00376G.

[19] Zhang, F., Jin, Y., Shi, J., Zhong, Y., Zhu, W., El-Shall, M.S. (2015). Polyoxometalates confined in the mesoporous cages of metal–organic framework MIL-100(Fe): Efficient heterogeneous catalysts for esterification and acetalization reactions. *Chemical Engineering Journal*, 269, 236–244. DOI: 10.1016/j.cej.2015.01.092.

[20] Yati, I., Pentimalli, M., Padela, F. (2022). Synthesis of high surface area copper trimesate MOF via mechanochemical method. *AIP Conference Proceedings*, 2493(1), 060008. DOI: 10.1063/5.0110018.

[21] Głowniak, S., Szczęśniak, B., Choma, J., Jaroniec, M. (2021). Mechanochemistry: Toward green synthesis of metal–organic frameworks. *Materials Today*, 46, 109–124. DOI: 10.1016/j.mattod.2021.01.008.

[22] Kumar, S., Jain, S., Nehra, M., Dilbaghi, N., Marrazza, G., Kim, K.-H. (2020). Green synthesis of metal–organic frameworks: A state-of-the-art review of potential environmental and medical applications. *Coordination Chemistry Reviews*, 420, 213407. DOI: 10.1016/j.ccr.2020.213407.

[23] Seetharaj, R., Vandana, P. V, Arya, P., Mathew, S. (2019). Dependence of solvents, pH, molar ratio and temperature in tuning metal organic framework architecture. *Arabian Journal of Chemistry*, 12(3), 295–315. DOI: 10.1016/j.arabjc.2016.01.003.

[24] Akhbari, K., Morsali, A. (2011). Effect of the guest solvent molecules on preparation of different morphologies of ZnO nanomaterials from the [Zn2(1,4-bdc)2(dabco)] metal-organic framework. *Journal of Coordination Chemistry*, 64(20), 3521–3530. DOI: 10.1080/00958972.2011.623778.

[25] Yang, D., Gates, B.C. (2019). Catalysis by Metal Organic Frameworks: Perspective and Suggestions for Future Research. *ACS Catalysis*, 9(3), 1779–1798. DOI: 10.1021/acscatal.8b04515.

[26] Han, Q., Wang, Z., Chen, X., Jiao, C., Li, H., Yu, R. (2019). Facile Synthesis of Fe-based MOFs(Fe-BTC) as Efficient Adsorbent for Water Purifications. *Chemical Research in Chinese Universities*, 35(4), 564–569. DOI: 10.1007/s40242-019-8415-z.

[27] Mazaj, M., Birsa Čelič, T., Mali, G., Rangus, M., Kaučič, V., Zabukovec Logar, N. (2013). Control of the Crystallization Process and Structure Dimensionality of Mg–Benzene–1,3,5-Tricarboxylates by Tuning Solvent Composition. *Crystal Growth & Design*, 13(8), 3825–3834. DOI: 10.1021/cg400929z.

[28] Majano, G., Pérez-Ramírez, J. (2013). Scalable Room-Temperature Conversion of Copper(II) Hydroxide into HKUST-1 (Cu3(btc)2). *Advanced Materials*, 25(7), 1052–1057. DOI: 10.1002/adma.201203664.

[29] Medina-Velazquez, D.Y., Caldiño, U., Morales-Ramirez, A., Reyes-Miranda, J., Lopez, R.E., Escudero, R., Ruiz-Guerrero, R., Morales Perez, M.F. (2019). Synthesis of luminescent terbium-thenoyltriflouroacetone MOF nanorods for green laser application. *Optical Materials*, 87, 3–10. DOI: 10.1016/j.optmat.2018.08.021.

[30] Satya, A.D.M., Zulys Agustino, Saepudin, E. (2022). Green synthesis of iron based metal-organic framework by microwave and its potential as drug delivery system. *AIP Conference Proceedings*, 2391(1), 050002. DOI: 10.1063/5.0072883.

[31] Li, Y., Tang, Z., Chen, C. (2021). The Modulating Effect of Ethanol on the Morphology of a Zr-Based Metal–Organic Framework at Room Temperature in a Cosolvent System. *Crystals*, 11(4) DOI: 10.3390/cryst11040434.

[32] Kevat, S., Lad, V.N. (2023). Green synthesis of zirconium-based MOF-808 by utilizing sustainable synthesis approaches. *Journal of Organometallic Chemistry*, 999, 122832. DOI: 10.1016/j.jorganchem.2023.122832.

[33] Zhang, B., Zhang, J., Liu, C., Sang, X., Peng, L., Ma, X., Wu, T., Han, B., Yang, G. (2015). Solvent determines the formation and properties of metal–organic frameworks. *RSC Adv*, 5(47), 37691–37696. DOI: 10.1039/C5RA02440D.

[34] Byrne, F.P., Jin, S., Paggiola, G., Petchey, T.H.M., Clark, J.H., Farmer, T.J., Hunt, A.J., Robert McElroy, C., Sherwood, J. (2016). Tools and techniques for solvent selection: green solvent selection guides. *Sustainable Chemical Processes*, 4(1), 7. DOI: 10.1186/s40508-016-0051-z.

[35] Mendiburu, A.Z., Lauermann, C.H., Hayashi, T.C., Mariños, D.J., Rodrigues da Costa, R.B., Coronado, C.J.R., Roberts, J.J., de Carvalho, J.A. (2022). Ethanol as a renewable biofuel: Combustion characteristics and application in engines. *Energy*, 257, 124688. DOI: 10.1016/j.energy.2022.124688.

[36] Canioni, R., Roch-Marchal, C., Sécheresse, F., Horcajada, P., Serre, C., Hardi-Dan, M., Férey, G., Grenèche, J.-M., Lefebvre, F., Chang, J.-S., Hwang, Y.-K., Lebedev, O., Turner, S., Van Tendeloo, G. (2011). Stable polyoxometalate insertion within the mesoporous metal organic framework MIL-100(Fe). *J. Mater. Chem.*, 21(4), 1226–1233. DOI: 10.1039/C0JM02381G.

[37] Bavykina, A., Kolobov, N., Khan, I.S., Bau, J.A., Ramirez, A., Gascon, J. (2020). Metal–Organic Frameworks in Heterogeneous Catalysis: Recent Progress, New Trends, and Future Perspectives. *Chemical Reviews*, 120 (16), 8468–8535. DOI: 10.1021/acs.chemrev.9b00685.

[38] Fadilah, C., Kurniawan, C., Ridwan, M., Al Muttaqii, M., Agustian, E., Andreani, A.S., Dwiatmoko, A.A., Yati, I. (2023). Synthesis of superacid sulfated TiO2 nanowires for esterification of waste cooking oil. *Reaction Kinetics, Mechanisms and Catalysis*, 136 (3), 1529–1544. DOI: 10.1007/s11144-023-02401-3.

[39] Sanchez-Sanchez, M., de Asua, I., Ruano, D., Diaz, K. (2015). Direct Synthesis, Structural Features, and Enhanced Catalytic Activity of the Basolite F300-like Semiamorphous Fe-BTC Framework. *Crystal Growth & Design*, 15 (9), 4498–4506. DOI: 10.1021/acs.cgd.5b00755.